International Journal of Bifurcation and Chaos, Vol. 26, No. 14 (2016) 1650232 (8 pages)

DOI: 10.1142/S0218127416502321

From Geodesic Flow on a Surface of Negative Curvature to Electronic Generator of Robust Chaos

Sergey P. Kuznetsov
Kotel'nikov's Institute of Radio-Engineering and Electronics of RAS, Saratov Branch, Zelenaya 38, Saratov 410019, Russia
spkuz@yandex.ru

Received May 12, 2016; Revised September 13, 2016

Departing from the geodesic flow on a surface of negative curvature as a classic example of the hyperbolic chaotic dynamics, we propose an electronic circuit operating as a generator of rough chaos. Circuit simulation in NI Multisim software package and numerical integration of the model equations are provided. Results of computations (phase trajectories, time dependencies of variables, Lyapunov exponents and Fourier spectra) show good correspondence between the chaotic dynamics on the attractor of the proposed system and of the Anosov dynamics for the original geodesic flow.

Keywords: Chaos; attractor; hyperbolicity; Anosov's dynamics; electronic circuit.

1. Introduction

The hyperbolic theory is a part of the theory of dynamical systems delivering a rigorous justification of the possibility of chaotic behavior of deterministic systems both for the discrete-time case (iterative maps — diffeomorphisms) and for the continuous time case (flows) [Smale, 1967; Shilnikov, 1997; Anosov *et al.*, 1995; Hasselblatt & Katok, 2003; Sinaĭ, 1981]. The objects of study are uniformly hyperbolic invariant sets in the phase space composed exclusively of saddle trajectories. For conservative systems, the hyperbolic chaos is represented by the Anosov dynamics when the uniformly hyperbolic invariant set either occupies a compact phase space (for diffeomorphisms), or occupies completely a surface of constant energy (for flows). For dissipative systems, the hyperbolic theory introduces a special kind of attracting invariant sets, the uniformly hyperbolic chaotic attractors.

A fundamental mathematical fact [Smale, 1967; Shilnikov, 1997; Anosov *et al.*, 1995; Hasselblatt & Katok, 2003] is that the uniformly hyperbolic invariant sets possess the property of roughness, or structural stability.

The word "roughness" is a translation of the Russian term from the seminal work of Andronov and Pontryagin [1937] referring the property of dynamical systems to keep up the qualitative behavior under small evolution operator variations: for any small deviation given by a differentiable function, a properly chosen continuous change of variables transforms the phase trajectories of the perturbed system to those of the original one. Later, in mathematical works, this property got a name of structural stability, commonly accepted now.

Initially introduced, the concept of roughness served as a strong basis for the development of nonlinear science; in particular, in the theory of oscillations, at least for systems with regular (nonchaotic) behavior, it is normally postulated that just the rough systems are of the main theoretical and practical interest [Andronov *et al.*, 1966]. In the case of chaotic dynamics this approach is really good only for systems with hyperbolic chaos, but it excludes majority of natural and technical examples of

chaotic motions. As a palliative, in physically oriented works people speak on the robust chaos meaning that chaotic nature of the dynamics persists under variations of parameters in some range [Banerjee *et al.*, 1998; Elhadj & Sprott, 2011], although the rigorous requirements of the structural stability (equivalence in respect to the variable changes) usually do not hold.

The use of the term "structural stability" certainly looks preferable as we want to accentuate the mathematical context (the trajectory equivalence for perturbed systems). Oppositely, the term "roughness" outlines rather a physical aspect, emphasizing the robustness of chaos, but for hyperbolic dynamical systems, it is especially appropriate as for them the roughness is properly perceived as equivalent to the structural stability.

The rough systems should be of preferable interest to any practical application of dynamical chaos due to insensitivity to variation of parameters, manufacturing imperfections, interferences, etc. (This point is outlined e.g. in [Dmitriev *et al.*, 2012].) Having in hand no examples "ready-for-use" from nature and technology, it makes sense to turn to the purposeful constructing systems with the hyperbolic dynamics appealing to tools of physics and electronics [Kuznetsov, 2011, 2012] exploiting naturally the roughness (structural stability). Namely, taking a formal example of hyperbolic dynamics as a prototype, one can try to modify it in such a way that the dynamical equations become associated with a physical system, hoping that, due to the roughness, the hyperbolic nature of the dynamics will survive this transformation. In this article, departing from the classical problem relating to a geodesic flow on a surface of negative curvature, we propose an electronic device that operates as a generator of robust chaos.

2. Geodesic Flow with Anosov Dynamics

It is known that free mechanical motion of a particle on a curved surface is carried out along the geodesic lines of the metric, which is defined by the quadratic form, expressing the kinetic energy W via the generalized velocities with coefficients depending on coordinates [Anosov, 1967; Balazs & Voros, 1986]. In the case of negative curvature, the motion is characterized by instability with respect to transverse perturbations. Therefore, if it occurs in a compact domain, it appears to be chaotic.

As an example, consider the geodesic flow on the so-called Schwarz primitive surface [Meeks & Pérez, 2012], which is defined in the three-dimensional space $(\theta_1, \theta_2, \theta_3)$ by the equation

$$\cos\theta_1 + \cos\theta_2 + \cos\theta_3 = 0, \tag{1}$$

and the motion takes place with constant kinetic energy

$$W = \frac{1}{2}(\dot\theta_1^2 + \dot\theta_2^2 + \dot\theta_3^2). \tag{2}$$

Here the mass is taken as a unit, and the relation (1) may be regarded as the imposed holonomic mechanical constraint. Because of the periodicity in three axes, the variables $\theta_{1,2,3}$ may be defined modulo 2π, and we can interpret the motion as proceeding in a compact domain, the cubic cell of size 2π.

For curvature in this case we obtain an explicit expression [Hunt & MacKay, 2003; Kuznetsov, 2015a, 2015b]:

$$K = -\frac{1}{2}\frac{\cos^2\theta_1 + \cos^2\theta_2 + \cos^2\theta_3}{(\sin^2\theta_1 + \sin^2\theta_2 + \sin^2\theta_3)^2}. \tag{3}$$

With the exception of eight points, where the numerator is zero, the curvature K is everywhere negative, so the geodesic flow implements the Anosov dynamics.

Mechanical motions associated with the geodesic flow on the surface (1) occur, for example, in the triple linkage system of Thurston–Weeks–MacKay–Hunt [Thurston & Weeks, 1984; Hunt & MacKay, 2003] in some special asymptotic case [Hunt & MacKay, 2003; Kuznetsov, 2015a, 2015b]. Also such dynamics are of interest in the context of model description of motion of particles in three-dimensional periodic potentials [Hunt & MacKay, 2003; Kozlov, 1997].

Using the standard procedure for mechanical systems with holonomic constraints [Goldstein *et al.*, 2001], we can write down the equations of motion in the form

$$\ddot\theta_1 = -\Lambda\sin\theta_1, \quad \ddot\theta_2 = -\Lambda\sin\theta_2, \quad \ddot\theta_3 = -\Lambda\sin\theta_3, \tag{4}$$

where the Lagrange multiplier Λ has to be determined by taking into account the algebraic condition of mechanical constraint complementing the

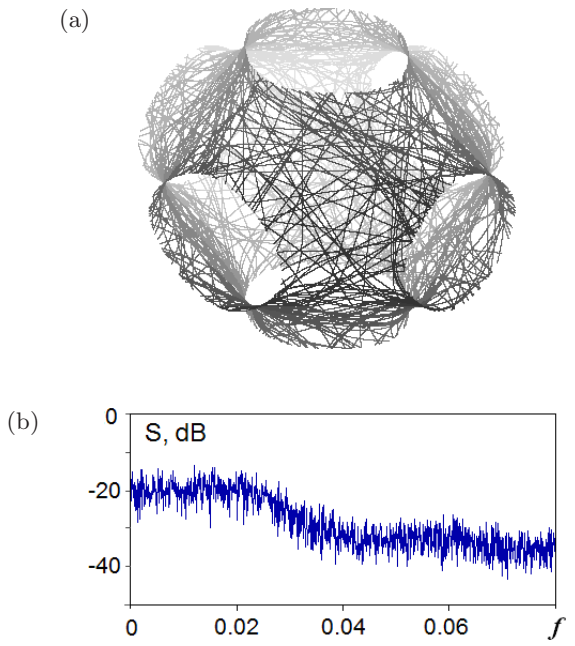

Fig. 1. (a) Typical trajectory of the system (4), (5) in a three-dimensional configuration space (θ_1, θ_2, θ_3) and (b) power spectrum of the variable $\dot{\theta}_1$ for the motion with the kinetic energy $W = 0.0425$. Plotting the diagram (a) the angular variables are related to the interval from 0 to 2π, i.e. it corresponds to a single fundamental cell, which is repeated with period 2π along each of the three coordinate axes.

differential equations. In our case

$$\Lambda = \frac{\dot{\theta}_1^2 \cos\theta_1 + \dot{\theta}_2^2 \cos\theta_2 + \dot{\theta}_3^2 \cos\theta_3}{\sin^2\theta_1 + \sin^2\theta_2 + \sin^2\theta_3}. \qquad (5)$$

Figure 1(a) shows a typical trajectory in the configuration space, which travels on the two-dimensional surface (1). The opposite faces of the cubic cell are naturally identified; resulting in a compact manifold of genus 3. In other words, the surface is topologically equivalent to the "pretzel with three holes" [Thurston & Weeks, 1984; Hunt & MacKay, 2003]. Visually, one can conclude about the chaotic nature of the trajectory covering the surface in ergodic manner. The power spectrum of the signal generated by the motion of the system is continuous, which is an intrinsic feature of chaos [Fig. 1(b)].

Taking into account the imposed mechanical constraint, there are four Lyapunov exponents characterizing the behavior of perturbations about the reference phase trajectory: one positive, one negative and two zero. One exponent equal to zero appears due to the autonomous nature of the system; it corresponds to the perturbation vector tangent to the phase trajectory. Another one is associated with a disturbance of energy. Since the system does not possess any certain characteristic time scale, the Lyapunov exponents responsible for the exponential growth or decay of perturbations are proportional to the velocity, i.e. $\lambda = \pm\kappa\sqrt{W}$, where the coefficient is determined by the average curvature of the metric. Empirically, from computations for the system under consideration $\kappa = 0.70$ [Kuznetsov, 2015a, 2015b].

3. Constructing Electronic Chaos Generator

In [Kuznetsov, 2015b] a self-oscillating system was suggested, where the sustained dynamical behavior corresponds approximately to the geodesic flow on the Schwarz surface; there the kinetic energy is not constant but undergoes some irregular fluctuations around a certain average level in the course of the dynamics in time. This system is based on three self-rotators, the elements whose state is defined by the angular variables $\theta_{1,2,3}$ and generalized velocities $\dot{\theta}_{1,2,3}$, and the steady motion of one element in isolation corresponds to the rotation in either direction with a certain constant angular velocity. The rotators are supposed to interact via the potential that is minimal under the condition (1). According to [Kuznetsov, 2015b], in a certain range of parameters the dynamics are hyperbolic, although for the modified system one should speak about self-oscillatory chaotic regimes corresponding to hyperbolic attractors rather than the Anosov dynamics. The purpose of this article is to propose an electronic circuit implementation of such system and to demonstrate its functioning as a generator of robust chaos.[1]

[1]It is worth stressing specially that it is not an attempt to construct an electronic circuit with conservative dynamics, which obviously could not result in a practically reasonable device because of the fact that conservative systems are atypical in framework of the entire class of dynamical systems. Actually, the aim is to get an electronic analog of a dissipative self-oscillatory system with rough chaos governed by a set of differential equations proposed in [Kuznetsov, 2015b]. Compliance of the dynamics on the attractor of that system to the dynamics of the geodesic flow on the Schwarz surface (Sec. 2) has been clearly demonstrated numerically [Kuznetsov, 2015b].

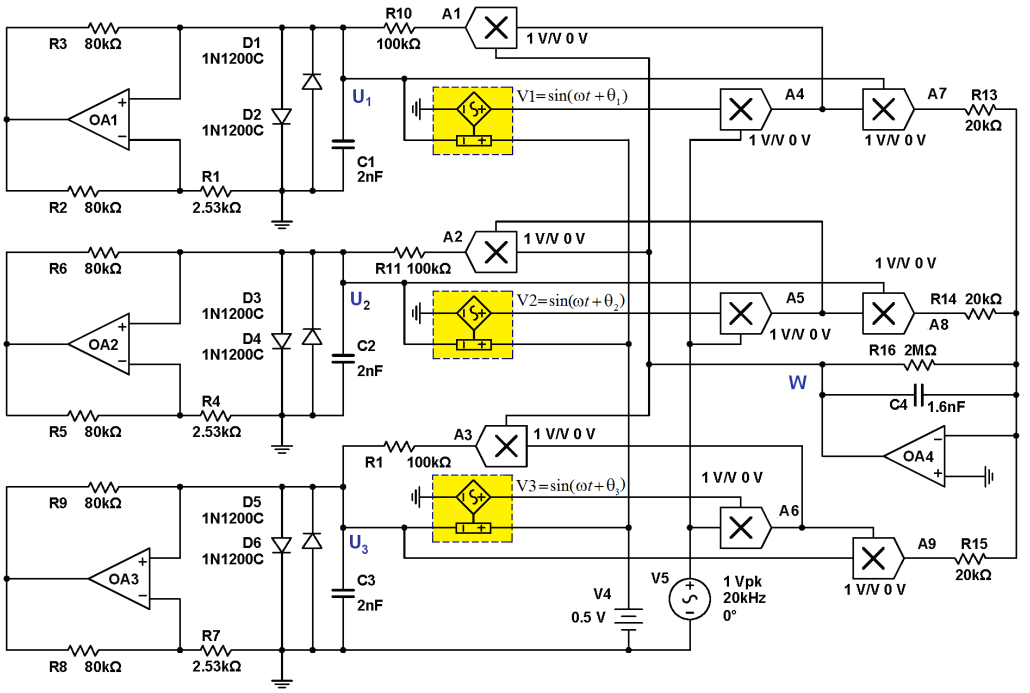

Fig. 2. Circuit diagram of the chaos generator composed with the NI Multisim software package. Boxes colored in yellow point out the voltage controlled oscillators V1, V2, V3 , which are the key components for the system functioning. The angular variables $\theta_1, \theta_2, \theta_3$ correspond to phases of these oscillators as indicated by the nearby inscriptions in the circuit diagram. Coefficients of the frequency control for V1, V2, V3 are equal to $k/2\pi = 40\,\mathrm{kHz/V}$.

For constructing the electronic device, elements are needed similar to rotators in mechanics. Namely, a state of the element has to be characterized by a generalized coordinate defined modulo 2π. An appropriate variable of such kind is a phase shift in the voltage controlled oscillator relative to a reference signal, like it is practiced in the phase-locked loops [Best, 2007].

Let us turn to the circuit diagram shown in Fig. 2. The voltages $U_{1,2,3}$ are used to control the phases of the oscillators V1, V2, V3, so that the voltage outputs vary in time as $\sin(\omega t + \theta_{1,2,3})$, where the phases satisfy the equations $\dot\theta_i = kU_i$, $i = 1, 2, 3$, and k is the coefficient characterizing the frequency control. The center frequency of the oscillators is determined by the bias provided by DC voltage source V4. The reference signal is generated by the AC voltage source V5.

Assuming the output voltages of the multipliers A1, A2, A3 to be $W_{1,2,3}$, for currents through the capacitors C1, C2, C3 we have $C\dot U_i + (R^{-1} - g)U_i + \alpha U_i + \beta U_i^3 = R^{-1}W_i$, where $i = 1, 2, 3$, $C = \mathrm{C1} = \mathrm{C2} = \mathrm{C3}$, $R = \mathrm{R10} = \mathrm{R11} = \mathrm{R12}$, and $I(U) = \alpha U + \beta U^3$ is approximation for the current–voltage characteristic of the nonlinear element composed of a pair of the diodes shown in Fig. 3. The equations take into account the negative conductivity $g = R_2/R_1R_3 = R_5/R_4R_6 = R_8/R_7R_9$ introduced by the blocks composed with the operation amplifiers OA1, OA2, OA3. The voltages $W_{1,2,3}$ are obtained by multiplying the signals $\sin(\omega t + \theta_{1,2,3})\cos\omega t$ from outputs of A4, A5, A6 by an output signal W of the inverting summing-integrating element containing the operational amplifier OA4.

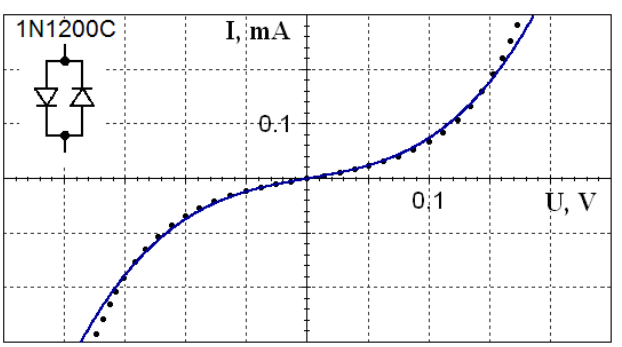

Fig. 3. The current–voltage characteristic of a nonlinear element composed of two parallel-connected diodes 1N1200C. The differential resistance at low voltage is $2.602\,\Omega$. Dots represent the data of the NI Multisim simulation, and the curve corresponds to the approximation $I(U) = \alpha U + \beta U^3 = 0.0039U + 0.035U^3$, where the current is expressed in amperes and voltage in volts.

Input signals for the summing-integrating element are the output voltages of the multipliers A7, A8, A9, so, that on account of the leakage current through the resistor R16, we have

$$C_0\dot{W} + r^{-1}W = -R_0^{-1}[U_1\sin(\omega t+\theta_1) + U_2\sin(\omega t+\theta_2) + U_3\sin(\omega t+\theta_3)]\cos\omega t,$$

where $C_0 = \mathrm{C4}$, $R_0 = \mathrm{R13} = \mathrm{R14} = \mathrm{R15}$, $r = \mathrm{R16}$.

Using variables $\tau = t/\sqrt{4RCR_0C_0}$, $u_i = 2k\sqrt{RCR_0C_0}U_i$, $w = 2kR_0C_0W$ and parameters $\Omega = \sqrt{4RCR_0C_0}\omega$, $\mu = (gR-\alpha R-1)\sqrt{4R_0C_0/RC}$, $\nu = \beta/\sqrt{4k^4RC^3R_0C_0}$, $\gamma = \sqrt{4RCR_0/r^2C_0}$, we rewrite the equations in dimensionless form, where the dot means now the derivative over τ:

$$\begin{aligned}\dot{\theta}_i &= u_i, \quad i = 1,2,3,\\ \dot{u}_i &= \mu u_i - \nu u_i^3 + 2w\sin(\Omega\tau+\theta_i)\cos\Omega\tau,\\ \dot{w} &= -\gamma w - 2\sum_{i=1}^{3} u_i\sin(\Omega\tau+\theta_i)\cos\Omega\tau.\end{aligned} \tag{6}$$

Nontrivial self-oscillatory behavior takes place at $\mu > 0$; this parameter may be varied by simultaneous tuning of the resistances R1, R4, R7, which are supposed to be identical.

Taking into account that $\Omega \gg 1$ one can simplify the equations assuming that u_i and w vary slowly on the high-frequency period. Namely, we perform averaging in the right-hand parts setting

$$\overline{\sin(\Omega\tau+\theta_i)\cos\Omega\tau} = \frac{1}{2}\sin\theta_i \tag{7}$$

and arrive at the equations

$$\begin{aligned}&\dot{\theta}_i = u_i, \quad \dot{u}_i = \mu u_i - \nu u_i^3 + w\sin\theta_i, \quad i = 1,2,3,\\ &\dot{w} = -\gamma w - (u_1\sin\theta_1 + u_2\sin\theta_2 + u_3\sin\theta_3).\end{aligned} \tag{8}$$

Finally, supposing $\gamma \ll 1$ we can neglect the respective term in the last equation and to integrate it with substitution of $u_{1,2,3}$ from the first equation; then we obtain $w \approx \cos\theta_1 + \cos\theta_2 + \cos\theta_3$, and the final result corresponds exactly to the equations in [Kuznetsov, 2015b]:

$$\ddot{\theta}_i = \mu\dot{\theta}_i - \nu\dot{\theta}_i^3 + (\cos\theta_1 + \cos\theta_2 + \cos\theta_3)\sin\theta_i, \quad i = 1,2,3. \tag{9}$$

4. Dynamic Simulation and Analysis

Figure 4 shows a sample of the signal U_1 copied from the virtual oscilloscope screen when simulating the dynamics of the circuit in the NI Multisim software package, and the spectrum obtained with the virtual spectrum analyzer. Visually, the signal looks chaotic, without any apparent repetition of forms.[2] Continuous spectrum corresponds to the chaotic nature of the process. It is characterized by slow decrease of the spectral density with frequency and is of rather good quality in the sense of lack of pronounced peaks and dips.

In a frame of the circuit simulation it is difficult to explore some characteristics, such as Lyapunov exponents, therefore, we turn to comparison of the results with the model (6), for which the relevant analysis in the computations can be performed. Using the component parameter values indicated in the circuit diagram of Fig. 2 and applying the conversion formulas to the dimensionless quantities, we evaluate the parameters in Eqs. (6): $\mu = 0.07497, \nu = 1.73156, \gamma = 0.05, \Omega = 20.1062$. Figure 5 shows a plot of the dimensionless variable u_1 versus time obtained from the numerical integration of Eqs. (6) in Fig. 5(a), and the Fourier spectrum in Fig. 5(b). The scales on the axes are chosen to provide correspondence with Fig. 4. Similar in form and characteristic scales are samples of time dependencies and spectra obtained for the models (8) and (9).

As one can see, the dynamics of the electronic device are similar to the original geodesic flow on the surface of negative curvature in the sense that the trajectories in the space of coordinate variables $(\theta_1, \theta_2, \theta_3)$ are close to the Schwarz surface. This is illustrated in Fig. 6, which shows a trajectory found by numerical integration of the equations for the model (6), and a diagram obtained from the data of circuit simulation in Multisim. To plot the last one, the circuit was complemented by three special signal processing modules. The output signal of each of the voltage controlled oscillators were subjected

[2]It occurs that the system startup may be accompanied by a very long-time transient to arrive at the attractor. It is easy to skip it in the course of numerical integration of the dynamical equations, but it is rather hard in a framework of the Multisim simulation. Shown in Figs. 4 and 5 waveforms relate to the dynamics on the attractor, with excluded transients.

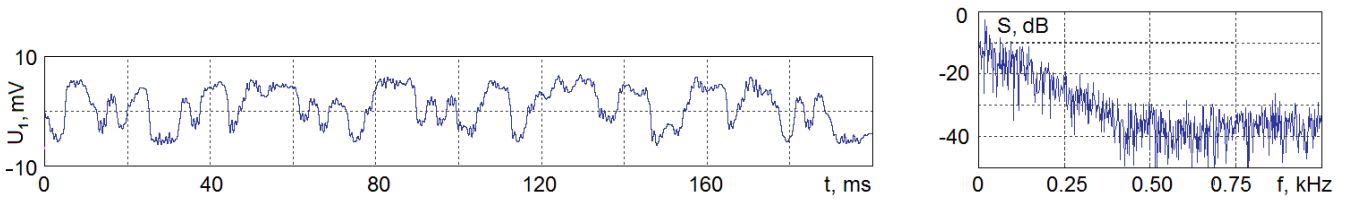

(a) (b)

Fig. 4. (a) Voltage on capacitor C1 versus time in a sustained regime and (b) its power spectrum as obtained by circuit simulation in Multisim.

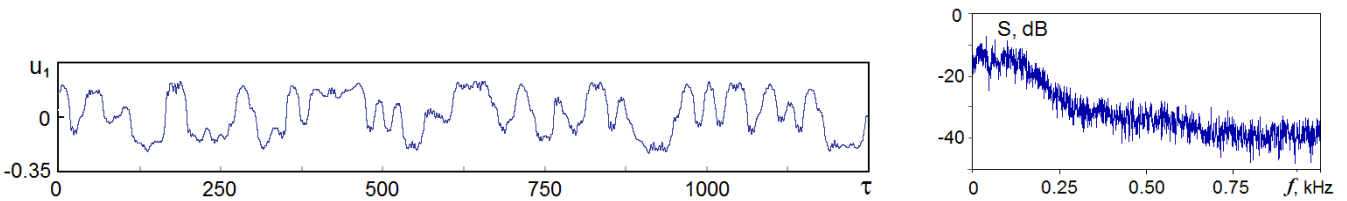

(a) (b)

Fig. 5. (a) Time dependence and (b) spectrum of the variable u_1 obtained from numerical integration of Eqs. (6).

to multiplication by $\sin\omega t$ and $\cos\omega t$, and after filtration and separation of the low-frequency components, three pairs of the resulting signals $(x_k,\ y_k)$, $k = 1, 2, 3$ were recorded in a file for subsequent processing. According to the recorded data, at each time point three variables defined modulo 2π are evaluated as $\theta_k = \arg(x_k + iy_k)$, $k = 1, 2, 3$, and respective points are plotted. These diagrams can be compared with Fig. 1 for the geodesic flow on the surface of negative curvature. Figure 6 shows that the trajectory remains close to the Schwarz surface, though it is not located exactly on it; the pictures are "fluffed" in the transverse direction. This effect becomes more pronounced with increasing parameter μ, as we move away from the critical point of appearance of self-oscillations at $\mu = 0$.

It was verified both in the course of integration of the dynamical equations and in the Multisim simulations that slight variations of the circuit component parameter values do not violate the observed nature of the dynamics; it agrees with the expected property of roughness (structural stability).

Figure 7 shows plots for all seven Lyapunov exponents calculated using the traditional algorithm [Benettin *et al.*, 1980; Schuster & Just, 2005; Kuznetsov, 2012] for the model (6) depending on the parameter μ. In the presented range of μ we have one positive exponent, other two are close to

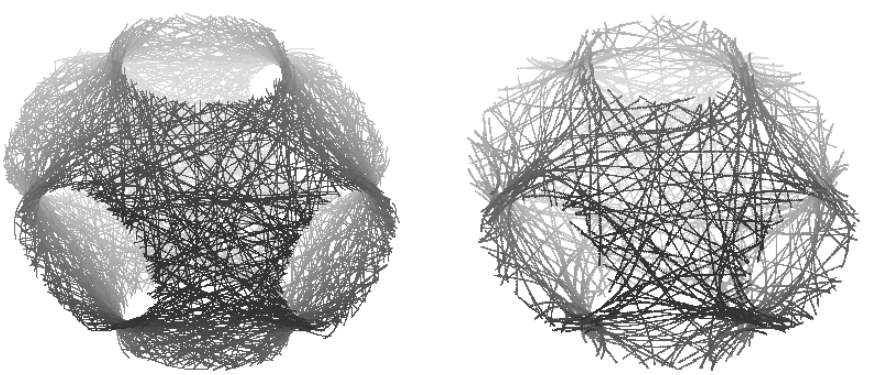

(a) (b)

Fig. 6. Trajectories in the three-dimensional space $(\theta_1, \theta_2, \theta_3)$ (a) for the model system (6) and (b) for the electronic device obtained from results of simulation in Multisim according to the method described in the text.

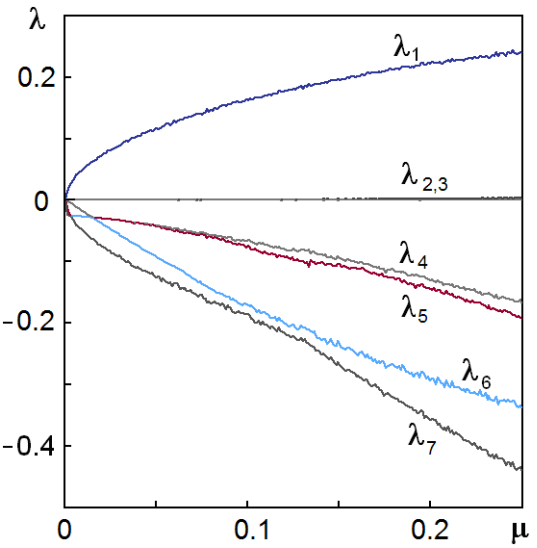

Fig. 7. Lyapunov exponents of the system (6) depending on the parameter of supercriticality μ.

zero, and the rest are negative.[3] The dependences on the parameter are smooth, without notable peaks and dips, testifying in favor of roughness of the chaotic attractor. Note that in [Kuznetsov, 2015b] special calculations were carried out based on verification of the absence of tangencies between stable and unstable subspaces of perturbation vectors nearby a typical trajectory on the attractor for the model (9); it argues in favor of assumption of the hyperbolic nature of the dynamics for the system under consideration.

Particularly, at $\mu = 0.07497$ the Lyapunov exponents of the attractor are

$$\lambda_1 = 0.1421 \pm 0.0012,$$

$$\lambda_2 = 0.0005 \pm 0.0003,$$

$$\lambda_3 = 0.0000 \pm 0.0002,$$

$$\lambda_4 = -0.0547 \pm 0.0006,$$

$$\lambda_5 = -0.0582 \pm 0.0009,$$

$$\lambda_6 = -0.1382 \pm 0.0004,$$

$$\lambda_7 = -0.1591 \pm 0.0022,$$

where errors indicated are the standard deviations obtained under averaging data for 10^2 samples of duration $\tau = 5 \cdot 10^4$. The averaged dimensionless kinetic energy in this case according to the computations is $W = \frac{1}{2}\overline{(u_1^2 + u_2^2 + u_3^2)} \approx 0.0425$, so, for the comparable geodesic flow the nonzero Lyapunov exponents should be equal to $\pm 0.7\sqrt{W} \approx \pm 0.144$; that agrees well with λ_1 and λ_7 relating to the model (6).

5. Conclusion

In this paper a construction of the electronic generator of rough chaos is proposed inspired by the geodesic flow on a surface of negative curvature, which implements hyperbolic dynamics of Anosov. An electronic analog circuit simulation is provided in the NI Multisim software package. Also, the set of equations is derived to describe the system, and computational study of chaotic dynamics is performed on the basis of these equations. In contrast to the previously considered electronic circuits with hyperbolic attractors [Kuznetsov, 2011, 2012; Isaeva *et al.*, 2015; Kuznetsov *et al.*, 2013], in this case the hyperbolicity is characterized by certain degree of uniformity in expansion and compression for elements of the phase volume in the course of evolution in continuous time. Thus, the generated chaos has rather good quality of the power spectral density distributions.

Although the particular circuit described in the article operates in the low-frequency range (kHz), it seems possible to implement similar devices at high frequencies as well.

Since the hyperbolic dynamics are characterized by roughness, or structural stability, as the mathematically proven attribute, it seems preferable for practical applications of chaos due to low sensitivity to parameter variations, various imperfections, noise, etc.

Acknowledgment

This work was partially supported by RFBR Grant No. 16-02-00135.

[3]It is worth commenting on the presence of two nearly zero Lyapunov exponents. In autonomous systems one exponent equal to zero always occurs being associated with a time-shift perturbation along the reference trajectory on the attractor. In our case, this is true for the reduced models (8) and (9). For the original system (6), which is periodically forced, one has to expect the respective exponent to be close to zero if the approximate description of the dynamics by means of the reduced model (8) is really good. (With the used parameters, this is just the case.) One more Lyapunov exponent close to zero appears because of the character of evolution of the variable w assumed in the device; in the secondary reduced model (9) it is excluded as may be checked in computations (see [Kuznetsov, 2015b]).

References

Andronov, A. A. & Pontryagin, L. S. [1937] "Systemes grossiers," *Dokl. Akad. Nauk SSSR* **14**, 247–250.

Andronov, A. A., Vitt, A. A. & Khaĭkin, S. Ė. [1966] *Theory of Oscillators* (Pergamon Press).

Anosov, D. V. [1967] "Geodesic flows on closed Riemannian manifolds of negative curvature," *Trudy Mat. Inst. Steklov* **90**, 3–210 (in Russian).

Anosov, D. V., Gould, G. G., Aranson, S. K., Grines, V. Z., Plykin, R. V., Safonov, A. V., Sataev, E. A., Shlyachkov, S. V., Solodov, V. V., Starkov, A. N. & Stepin, A. M. [1995] *Dynamical Systems IX*: *Dynamical Systems with Hyperbolic Behaviour*, Encyclopaedia of Mathematical Sciences, Vol. 9 (Springer).

Balazs, N. L. & Voros, A. [1986] "Chaos on the pseudosphere," *Trudy Mat. Inst. Steklov* **143**, 109–240.

Banerjee, S., Yorke, J. A. & Grebogi, C. [1998] "Robust chaos," *Phys. Rev. Lett.* **80**, 3049–3052.

Benettin, G., Galgani, L., Giorgilli, A. & Strelcyn, J.-M. [1980] "Lyapunov characteristic exponents for smooth dynamical systems and for Hamiltonian systems: A method for computing all of them," *Meccanica* **15**, 9–30.

Best, R. E. [2007] *Phase-Locked Loops*: *Design*, *Simulation and Applications*, 6th edition (McGraw-Hill).

Dmitriev, A. S., Efremova, E. V., Maksimov, N. A. & Panas, A. I. [2012] *Generation of Chaos* (Technosfera, Moscow) (in Russian).

Elhadj, Z. & Sprott, J. C. [2011] *Robust Chaos and Its Applications* (World Scientific, Singapore).

Goldstein, H., Poole Jr., Ch. P. & Safko, J. L. [2001] *Classical Mechanics*, 3rd edition (Addison-Wesley, Boston, Mass).

Hasselblatt, B. & Katok, A. A. [2003] *First Course in Dynamics*: *With a Panorama of Recent Developments* (Cambridge University Press).

Hunt, T. J. & MacKay, R. S. [2003] "Anosov parameter values for the triple linkage and a physical system with a uniformly chaotic attractor," *Nonlinearity* **16**, 1499–1510.

Isaeva, O. B., Kuznetsov, S. P., Sataev, I. R., Savin, D. V. & Seleznev, E. P. [2015] "Hyperbolic chaos and other phenomena of complex dynamics depending on parameters in a nonautonomous system of two alternately activated oscillators," *Int. J. Bifurcation and Chaos* **25**, 1530033-1–15.

Kozlov, V. V. [1997] "Closed orbits and chaotic dynamics of a charged particle in a periodic electromagnetic field," *Regul. Chaot. Dyn.* **2**, 3–12.

Kuznetsov, S. P. [2011] "Dynamical chaos and uniformly hyperbolic attractors: From mathematics to physics," *Phys. Uspekhi* **54**, 119–144.

Kuznetsov, S. P. [2012] *Hyperbolic Chaos*: *A Physicist's View* (Springer, Berlin; HEP, Beijing).

Kuznetsov, S. P., Ponomarenko, V. I. & Seleznev, E. P. [2013] "Autonomous system generating hyperbolic chaos: Circuit simulation and experiment," *Izvestiya VUZ. Appl. Nonlin. Dyn.* **21**, 17–30 (in Russian).

Kuznetsov, S. P. [2015a] "Chaos in the system of three coupled rotators: From Anosov dynamics to hyperbolic attractor," *Izv. Saratov. Univ.* (*N. S.*), *Ser. Fiz.* **15**, 5–17 (in Russian).

Kuznetsov, S. P. [2015b] "Hyperbolic chaos in self-oscillating systems based on mechanical triple linkage: Testing absence of tangencies of stable and unstable manifolds for phase trajectories," *Regul. Chaot. Dyn.* **20**, 649–666.

Meeks, W. H. & Pérez, J. [2012] *A Survey on Classical Minimal Surface Theory*, University Lecture Series, Vol. 60 (American Mathematical Society).

Schuster, H. G. & Just, W. [2005] *Deterministic Chaos*: *An Introduction* (Wiley-VCH).

Shilnikov, L. [1997] "Mathematical problems of nonlinear dynamics: A tutorial," *Int. J. Bifurcation and Chaos* **7**, 1353–2001.

Sinaĭ, Ya. G. [1981] "The stochasticity of dynamical systems," *Selected Translations*, *Selecta Math. Soviet.* **1**, 100–119.

Smale, S. [1967] "Differentiable dynamical systems," *Bull. Amer. Math. Soc.* (*NS*) **73**, 747–817.

Thurston, W. P. & Weeks, J. R. [1984] "The mathematics of three-dimensional manifolds," *Sci. Am.* **251**, 94–106.